Chapter Thirty-four

Physical Processes in Hot Gas

Within the Galaxy, hot ($T \gtrsim 10^6$ K) gas is produced by fast stellar winds, and by blastwaves from novae and supernovae. Beyond the Galaxy, much of the intergalactic medium is thought to be at $\sim 10^6$ K temperatures, and enormous masses of very hot ($10^7 - 10^8$ K) plasma are present in galaxy clusters. In some cases, the gas is detected via absorption lines of highly ionized species, such as O VI; in some cases, x-ray emission is observable.

In Chapter 25, we discussed the physics of dust grains immersed in hot gas. Here, we discuss gas-phase processes that affect the temperature of the gas: radiative cooling, thermal conduction, and electron–ion energy equipartition.

34.1 Radiative Cooling

Collisional excitation of ions in low-density plasma results in radiative cooling. The emitted power depends on the ionization state, and the plasma is often assumed to be in **collisional ionization equilibrium**, or **CIE**. CIE assumes that the plasma is in a steady state, and that collisional ionization, charge exchange, radiative recombination, and dielectronic recombination are the only processes altering the ionization balance, in which case the ionization fractions for each element depend only on the gas temperature, with no dependence on the gas density.

At temperatures $T > 10^4$ K, ionization of hydrogen provides enough free electrons so that collisional excitation of atoms or ions is dominated by electron collisions. At low densities, every collisional excitation is followed by a radiative decay, and the rate of removal of thermal energy per unit volume can therefore be written

$$\Lambda = n_e n_{\rm H} \times f_{\rm cool}(T) \; , \tag{34.1}$$

where the **radiative cooling function** $f_{\rm cool}(T) \equiv \Lambda / n_{\rm H} n_e$ is a function of temperature and of the elemental abundances relative to hydrogen.

At high densities, radiative cooling can be suppressed by collisional deexcitation, and $f_{\rm cool}$ will then depend on density $n_{\rm H}$, in addition to T and elemental abundances. Finally, if ionizing radiation is present, the ionization balance may depart from CIE, and the radiative cooling function $\Lambda / n_e n_{\rm H}$ will also depend on the spectrum and intensity of the ionizing radiation.

The cooling function $\Lambda / n_e n_{\rm H}$ for $T > 10^4$ K has been calculated by a number of groups over the years (e.g., Boehringer & Hensler 1989; Schmutzler & Tscharnuter

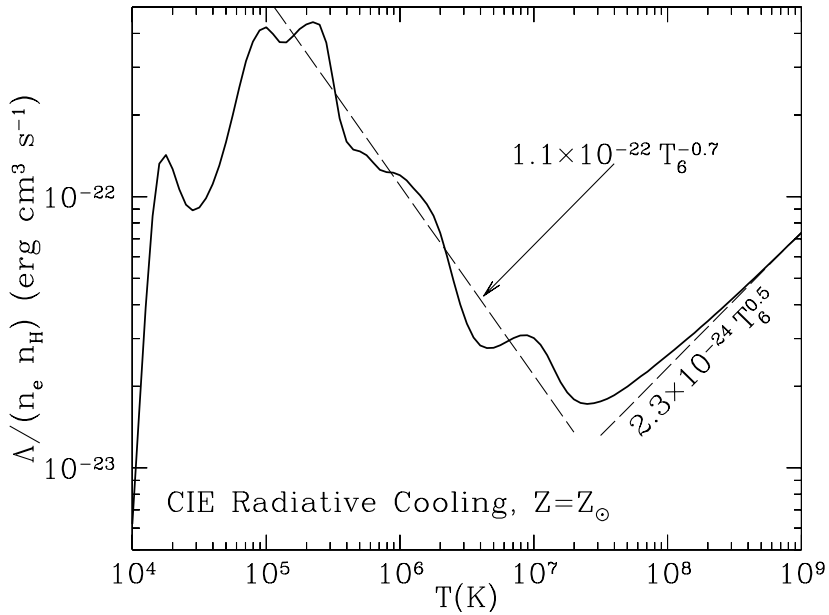

Figure 34.1 Radiative cooling function $\Lambda/n_e n_{\rm H}$ for solar-abundance plasma in CIE, computed with the CHIANTI code (Dere et al. 2009). Dashed lines show simple power-law approximations for $10^5 < T < 10^{7.3}$ K and for $T > 10^{7.5}$ K.

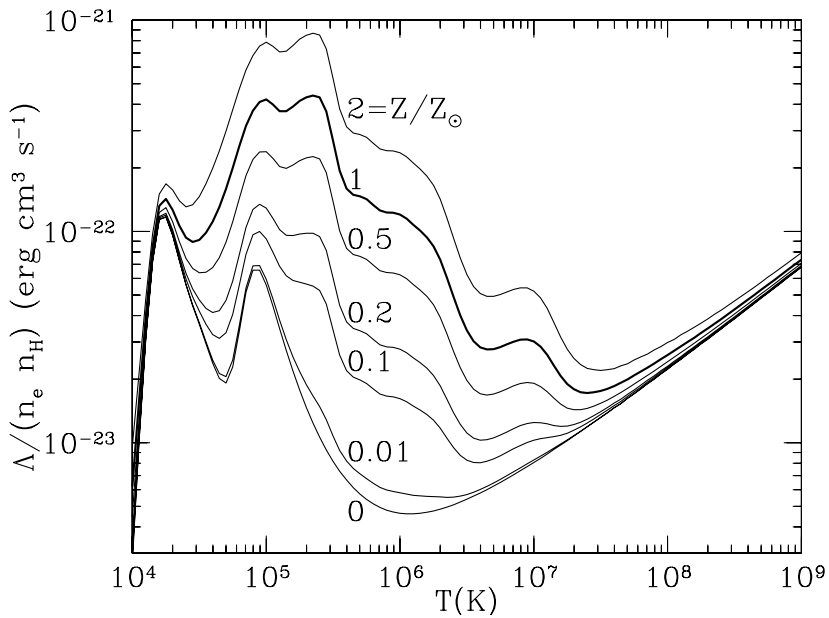

Figure 34.2 Same as Fig. 34.1, but for different abundances. $Z/Z_\odot$ is the abundance of elements heavier than He relative to solar abundances.

1993; Sutherland & Dopita 1993; Landi & Landini 1999; Smith et al. 2008; Dere et al. 2009; Schure et al. 2009). While the calculated cooling rates are in approximate agreement with one another, with some differences attributable to different adopted elemental abundances, there appear to also be significant differences in the adopted atomic physics. For example, near 10^5 K the cooling function of Schure et al. (2009) is a factor ~ 2.5 higher than the cooling function of Dere et al. (2009).

Figure 34.1 shows the radiative cooling function $\Lambda/n_{\rm H}n_e$ for plasma with solar abundances, based on calculations with the CHIANTI atomic database (Dere et al. 2009), kindly calculated for $n_{\rm H} = 1\,{\rm cm}^{-3}$ by K. Dere (2009, private communication). At temperatures $T < 10^7$ K, the cooling is dominated by collisional excitation of bound electrons. At high temperatures, the ions are fully stripped of electrons, and bremsstrahlung (i.e., free–free) cooling dominates, with $\Lambda/n_e n_{\rm H} \propto T^{0.5}$. The cooling function for solar abundances can be approximated by

$$\Lambda/n_e n_{\rm H} \approx 1.1 \times 10^{-22} T_6^{-0.7}\,{\rm erg\,cm^3\,s^{-1}}\ ,\ \text{for } 10^5 < T < 10^{7.3}\,{\rm K}\ , \quad (34.2)$$

$$\Lambda/n_e n_{\rm H} \approx 2.3 \times 10^{-24} T_6^{0.5}\,{\rm erg\,cm^3\,s^{-1}}\ , \quad \text{for } T > 10^{7.3}\,{\rm K}\ . \quad (34.3)$$

These two power-law fits are shown in Fig. 34.1.

In some cases (e.g., supernova ejecta), the plasma may have unusual abundance patterns, but in most applications the abundances of elements beyond He can be assumed to scale up and down together. Figure 34.2 shows radiative cooling functions for metallicities ranging from zero (H and He only) to twice solar.

Before using a rate coefficient for radiative cooling such as that shown in Figure 34.1, it is important to recognize its limitations:

- CIE requires that photoionization be unimportant.
- CIE requires that the plasma had time to attain collisional ionization equilibrium. If the gas has been suddenly shock-heated, time is required for collisional ionization to raise the ionization level to CIE. If the gas is cooling, the cooling rate should be slow enough that recombination processes are able to keep the ionization from lagging too far behind the ionization state corresponding to CIE.
- Figure 34.3 shows the contribution to the cooling from each of the 10 most important elements: H, He, C, N, O, Ne, Mg, Si, S, and Fe. For $10^{5.8} < T < 10^{7.2}$ K, radiative cooling is dominated by Mg, Si, and Fe – elements that in cold gas are normally depleted by factors of 5 or more. If these elements are underabundant in the plasma, the radiative cooling function will be suppressed. An accurate treatment of radiative cooling requires following the changing abundances in the gas phase as dust grains undergo sputtering in $T \gtrsim 10^6$ K plasma (see Fig. 25.4).
- In real problems, heating and cooling may be sufficiently rapid so that the ionization state of the gas lags behind CIE. This is particularly likely if the

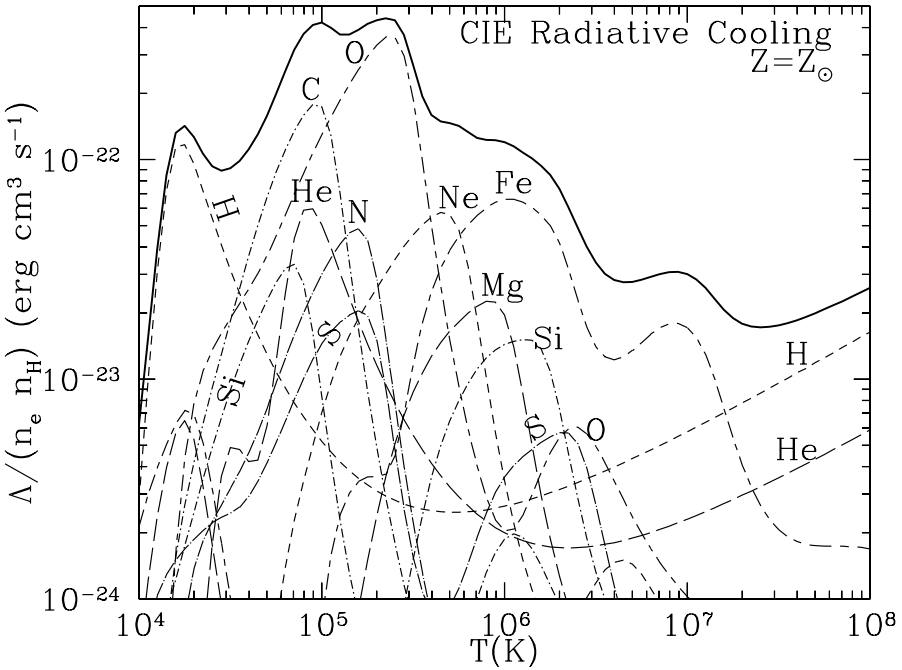

Figure 34.3 Solid line: radiative cooling function $\Lambda/n_e n_{\rm H}$ from Fig. 34.1, with contributions from selected elements shown.

gas has just been shock-heated, resulting in a sudden increase in the kinetic temperature of the gas, but can also be true when the gas is cooling rapidly, e.g., at $10^{4.9} < T < 10^{5.4}$ K, where the radiative cooling function peaks.

In these cases, the actual radiative cooling rate can be *slower* than CIE (when the gas is cooling faster than it can recombine, so that heavy elements have fewer bound electrons than they would in CIE), or *faster* than CIE (when the gas temperature has been suddenly increased, so that heavy elements are under-ionized). Underionization of elements such as Mg, Si, or Fe can also be an issue when atoms are being sputtered off of dust grains, since they are expected to enter the hot gas as neutral atoms.

34.2 Radiative Cooling Time

If the plasma cools at constant volume, the cooling time is given by Eq. (35.34). The cooling time is shown in Fig. 34.4 for metallicities ranging from 0 to 3 times

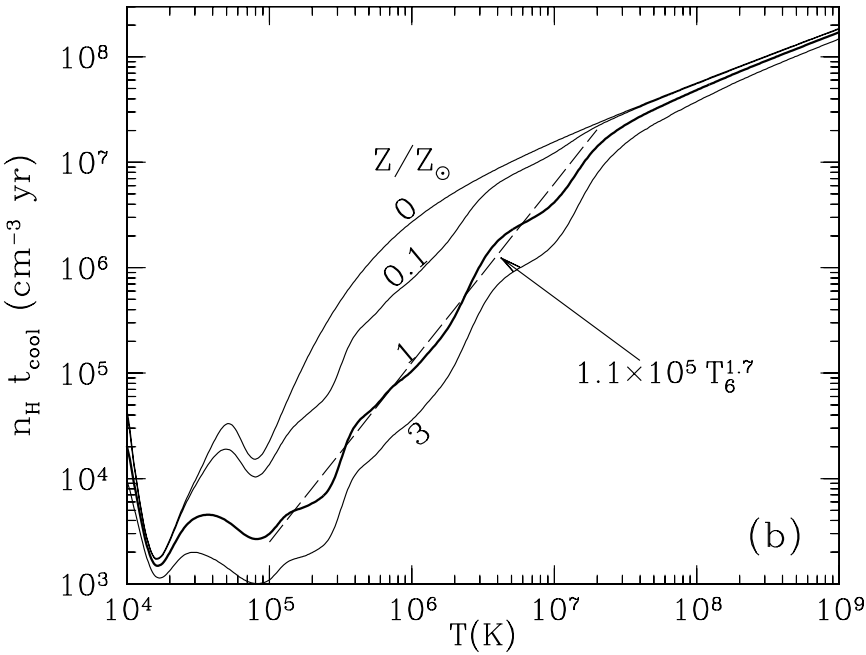

Figure 34.4 $n_{\rm H}t_{\rm cool,isochoric}$ for isochoric cooling with the cooling function from Fig. 34.1, for different metal abundances relative to solar. The dashed line is the approximation (34.4) for $Z \approx Z_\odot$ and $10^5\,{\rm K} < T < 10^{7.3}\,{\rm K}$.

solar. The cooling time for solar abundance plasma can be approximated by

$$\tau_{\rm cool,isochoric} \approx \frac{1.1\times10^5 T_6^{1.7}\,{\rm yr}}{n_{\rm H}/\,{\rm cm}^{-3}} \quad \text{for } 10^5\,{\rm K} \lesssim T \lesssim 10^{7.3}\,{\rm K} \quad . \tag{34.4}$$

34.3⋆ Thermal Conduction

In the absence of magnetic fields, a fully ionized H-He plasma has a "classical" thermal conductivity (Spitzer 1962):

$$\kappa_{\rm class}(T) \approx 0.87 \frac{k^{7/2}T_e^{5/2}}{m_e^{1/2}e^4\ln\Lambda} \quad , \tag{34.5}$$

where $\ln\Lambda \approx 30$ is the usual Coulomb logarithm, given by Eq. (2.17), and the numerical factor 0.87 includes the effects of the electric field that normally accompanies a temperature gradient in a uniform-pressure plasma (Spitzer 1962).

If a magnetic field is present, as is normally the case in the ISM, the thermal conductivity becomes a tensor. In a coordinate frame where $\mathbf{x} \parallel \mathbf{B}$, the thermal conductivity tensor is diagonal, with diagonal elements $(\kappa_\parallel, \kappa_\perp, \kappa_\perp)$, where $\kappa_\parallel = \kappa_{\rm class}$ The ratio $\kappa_\perp/\kappa_\parallel \approx 1/(\omega_B t_{\rm coll})^2$, where $\omega_B = eB/m_e c$ is the electron gyrofrequency, and $t_{\rm coll}$ is the mean collision time. For normal interstellar conditions, $\omega_B t_{\rm coll} \gg 1$, hence $\kappa_\perp \ll \kappa_\parallel$, and we need consider only the heat flow resulting from the component of ∇T along the local magnetic field direction.

When the temperature gradient becomes very large, the heat conduction "saturates," with the heat flux approaching a value $q_{\rm sat} \approx 5\rho(kT/\mu)^{3/2}$ (Cowie & McKee 1977). For finite ∇T, the heat flux can be written

$$\mathbf{q} \approx -\frac{\kappa_{\rm class} \nabla T \cdot \hat{\mathbf{b}}\hat{\mathbf{b}}}{1+\sigma_T} \quad , \tag{34.6}$$

where $\hat{\mathbf{b}} \equiv \mathbf{B}/|\mathbf{B}|$ is a unit vector parallel to the magnetic field, and the "saturation parameter"

$$\sigma_T \equiv \frac{\kappa_{\rm class}|\nabla T \cdot \hat{\mathbf{b}}|}{q_{\rm sat}} \tag{34.7}$$

$$= 2.53\,\frac{k^2\,T\,|\nabla T \cdot \hat{\mathbf{b}}|}{n_{\rm H}\,e^4\,\ln\Lambda} \tag{34.8}$$

$$= 0.39\left(\frac{T}{10^7\,{\rm K}}\right)\left(\frac{|\nabla T \cdot \hat{\mathbf{b}}|}{10^7\,{\rm K\,pc^{-1}}}\right)\left(\frac{{\rm cm^{-3}}}{n_{\rm H}}\right)\left(\frac{30}{\ln\Lambda}\right). \tag{34.9}$$

34.4⋆ Cloud Evaporation in Hot Gas

Consider now a cold spherical cloud, with temperature T_c and radius R_c, surrounded by very hot gas, with temperature $T_h \gg T_c$. Suppose that $T_h \gtrsim 10^6\,{\rm K}$, so that the rate coefficient for radiative cooling (see Fig. 34.1) is relatively low. What is the temperature profile near the cloud?

Let us first neglect radiative losses. Further assume that there is negligible heat flow into the cold cloud itself. Then, at each radius, the inward thermal conduction must be balanced by outward advective transport of heat. For a steady constant-pressure outward flow, mass conservation and energy conservation give

$$\frac{5\dot{M}kT}{2\mu} = -4\pi r^2 \kappa \frac{dT}{dr} \quad , \tag{34.10}$$

where $\dot{M}$ is the rate of mass flow out of the cloud. If we assume a thermal conduc-

tivity $\kappa = \kappa_h (T/T_h)^{5/2}$, then one finds

$$T = T_h \left(1 - \frac{R_c}{r}\right)^{2/5} \quad , \tag{34.11}$$

$$\dot{M} = \frac{16\pi\mu R_c \kappa_h}{25k} \propto R_c T_h^{5/2} \quad . \tag{34.12}$$

What about cooling? The temperature just outside the cloud surface must pass through $T \approx 10^5\,\mathrm{K}$ where the cooling function peaks (see Fig. 34.1). There are two limiting cases: (1) the small temperature gradient regime, where thermal conduction is small and cannot balance radiative cooling from the region where $T \approx 10^5\,\mathrm{K}$; and (2) the evaporative regime where radiative cooling is negligible, and there is an "evaporative flow" away from the cloud.

Cowie & McKee (1977) defined a "global saturation parameter":

$$\sigma_0 \equiv \frac{(2/25)\kappa_h T_h}{\rho_h (kT_h/\mu)^{3/2} R_c} = 0.4 \left(\frac{T_h}{10^7\,\mathrm{K}}\right)^2 \left(\frac{\mathrm{cm}^{-3}}{n_{\mathrm{H},h}}\right) \left(\frac{\mathrm{pc}}{R_c}\right) \tag{34.13}$$

and found three regimes:

$$\sigma_0 \lesssim 0.027 \quad : \text{cooling flow onto the cloud,} \tag{34.14}$$

$$0.027 \lesssim \sigma_0 \lesssim 1 \quad : \text{classical evaporation flow,} \tag{34.15}$$

$$1 \lesssim \sigma_0 \quad : \text{saturated evaporation flow.} \tag{34.16}$$

If we are in the regime $0.03 \lesssim \sigma_0 \lesssim 1$ where the classical evaporation mass loss rate (34.12) applies, the cloud lifetime against evaporation is

$$t_{\mathrm{evap}} = \frac{3M}{2\dot{M}} = \frac{75 \times 2.3\,(n_{\mathrm{H}})_c\, R_c^2\, m_e^{1/2}\, e^4 \ln\Lambda}{8 \times 0.87\,(kT_h)^{2.5}} \tag{34.17}$$

$$= 5.1 \times 10^4\,\mathrm{yr} \left(\frac{(n_{\mathrm{H}})_c}{30\,\mathrm{cm}^{-3}}\right) \left(\frac{R_c}{\mathrm{pc}}\right)^2 \left(\frac{T_h}{10^7\,\mathrm{K}}\right)^{-2.5} \quad . \tag{34.18}$$

Therefore, if the classical thermal conductivity applies, small ($R_c \lesssim 1\,\mathrm{pc}$) clouds will be thermally evaporated by hot ($T_h \gtrsim 10^7\,\mathrm{K}$) gas in a few $\times 10^4\,\mathrm{yr}$.

34.5⋆ Conduction Fronts

Earlier, we discussed a spherical cloud in an infinite medium. Other geometries yield different behavior. Consider a planar cold cloud brought suddenly into contact with an infinite region of hot gas. At $t = 0$, the temperature profile is a step function. The conduction front then begins to heat some of the cold gas, bringing

it to intermediate temperatures. As long as the front is thin, radiative losses are negligible compared to the heat flux into the intermediate temperature zone, and the continuing heat flux causes this intermediate temperature zone to grow. As the conduction front thickens and temperature gradients drop, the radiative losses increase, the conductive flux decreases, and the front approaches an asymptotic solution where evaporation ceases and thermal conduction is balanced by radiative losses.

If $T_h \gtrsim 10^6\,\mathrm{K}$, then the conduction front will contain ions such as C IV, Si IV, N V, S VI, and O VI, which have strong ultraviolet absorption lines that can be used as diagnostics. Borkowski et al. (1990) carried out simulations of planar conduction fronts including magnetic fields. The O VI abundance, for example, rises to $N(\mathrm{O\,VI}) \approx 10^{13}\,\mathrm{cm}^{-2}$ on a time scale of $\sim 10^5\,\mathrm{yr}$ if $\mathbf{B} = 0$ or if $\mathbf{B}$ is perpendicular to the interface. If a magnetic field is present and inclined to the normal, the conduction front becomes thinner, and the ionic column densities are reduced.